# Cavitation of electron bubbles in liquid parahydrogen

Francesco Ancilotto, Manuel Barranco, Jesús Navarro, Martí Pi

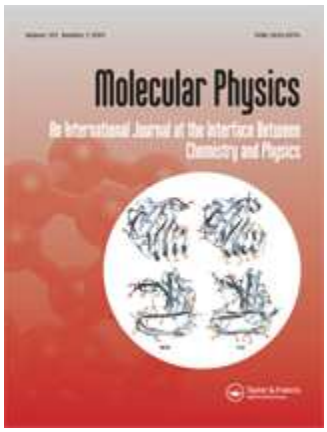


# Cavitation of electron bubbles in liquid parahydrogen

| | |
|---|---|
| Journal: | *Molecular Physics* |
| Manuscript ID: | TMPH-2011-0176 |
| Manuscript Type: | Special Issue in honour of Luciano Reatto |
| Date Submitted by the Author: | 08-Jun-2011 |
| Complete List of Authors: | Ancilotto, Francesco<br>Barranco, Manuel; Universitat de Barcelona, Facultat de Física, E.C.M.<br>Navarro, Jesús; IFIC, CSIC-University of Valencia<br>Pi, Martí; Universitat de Barcelona, Facultat de Física, E.C.M. |
| Keywords: | liquid parahydrogen, electron bubbles, density functional theory, capillary approximation |
| | |

*Molecular Physics*
Vol. 00, No. 00, 6 June 2011, 1–9

## INVITED ARTICLE

# *Cavitation of electron bubbles in liquid parahydrogen*

Francesco Ancilotto[a], Manuel Barranco[b*], Jesús Navarro[c] and Martí Pi[b]

[a] *Dipartimento di Fisica 'G. Galilei', Università di Padova, via Marzolo 8, I-35131 Padova, Italy and CNR-IOM-Democritos, I-34014 Trieste, Italy*; [b] *Departament ECM, Facultat de Física, and IN$^2$UB, Universitat de Barcelona. Diagonal 647, 08028 Barcelona, Spain*; [c] *IFIC (CSIC University of Valencia) Apartado 22085, 46071 Valencia, Spain*

(*June 2011*)

Within a finite-temperature density functional approach, we have investigated the structure of electron bubbles in liquid parahydrogen below the saturated vapor pressure, determining the critical pressure at which electron bubbles explode as a function of temperature. The electron-parahydrogen interaction has been modeled by a Hartree-type local potential fitted to the experimental value of the conduction band-edge for a delocalized electron in $pH_2$. We have found that the pressure for bubble explosion is, in absolute value, about a factor of two smaller than that of the homogeneous cavitation pressure in the liquid. Comparison with the results obtained within the capillary model shows the limitations of this approximation, especially as temperature increases.

**Keywords:** liquid parahydrogen; electron bubbles; density functional theory; capillary approximation



## 1. Introduction

Excess electrons in cryogenic liquids like helium and hydrogen have been the subject of many theoretical and experimental studies. It is well established that when an electron is injected into such liquids, it looses kinetic energy by ionization and excitation of the liquid atoms, and by the production of elementary excitations in the liquid. When the electron has lost most of its kinetic energy and moves subsonically, it eventually produces a cavity in the fluid and gets trapped inside it. We will refer to these structures as electron bubbles (e-bubbles). Many works have been devoted to measure the mobility of electron bubbles in liquid helium [1–4] and hydrogen [5–9].

In the case of helium, there is a wealth of experimental and theoretical work on heterogeneous cavitation produced by excess electrons when the fluid is driven below the saturated vapor pressure by the application of ultrasonic pulses caused by a transducer [10]. At given temperature ($T$), there is a limiting (critical) pressure below which electron bubbles explode triggering liquid-gas phase separation. In the case of helium, this process is well known and the agreement between theory and experiment is very satisfactory [11, 12].

It was theoretically predicted that electron bubbles should develop in liquid hydrogen [13], and they were experimentally detected shortly after [5]. Mobility experiments[14] disclosed an anomalously high mobility of negative charges in the

*Corresponding author. Email: manuel@ecm.ub.es

ISSN: 00268976 print/ISSN 13623028 online

DOI: 10.1080/0026897YYxxxxxxxx
http://www.informaworld.com

$T$ range from 17 to 22 K that was attributed to the existence of $H^-$ anions in the liquid, as discussed in detail in [7]. It thus appears that in liquid hydrogen two types of negatively charged bubbles may develop when electrons are injected inside it, i.e. ordinary e-bubbles and '$H^-$-bubbles'.

As compared with liquid helium, much less is known on cavitation caused by e-bubbles in liquid hydrogen. We have recently addressed homogeneous nucleation and cavitation in parahydrogen [15] ($pH_2$) using a zero-range finite-temperature density functional [16] (DF) that reproduces the properties of liquid $pH_2$ in the pressure ($P$) and $T$ ranges corresponding to the liquid-vapor phase equilibrium region, i.e., from the triple to the critical point. It was found that the spinodal pressure $P_{sp}$ near the triple point was about -80 bar, whereas the homogeneous cavitation pressure (that at which gas bubbles are created in the liquid at a rate large enough so as to trigger the liquid-vapor phase transition) in the same region of the phase diagram was about -70 bar. This value is very much affected by the presence of electrons (heterogeneous cavitation). Indeed, we have found [15] that in the triple point region the pressure for e-bubble explosion is just $P_{expl} \sim -30$ bar. That estimate was obtained within the capillary model that describes the electron bubble as a sharp spherical cavity and neglects the thickness of the cavity inner surface, whose width drastically increases as one approaches the critical point. As a result, in the capillary model approximation $P_{expl}$ eventually becomes more negative than $P_{sp}$, which is unphysical.

In this work we want to determine $P_{expl}$ more accurately by going beyond the crude capillary model. To this end, we resort to the finite-range density functional (FRDF) of [16], which has proven to accurately describe the temperature dependent, finite width of the liquid-vapor interface, supplementing it with an electron-$pH_2$ interaction obtained within a Hartree-type model, which has been successfuly used in the case of liquid helium [23]. This work is organized as follows. In Sec. 2 we present the conventional capillary approximation to electron bubbles in cryogenic fluids. The density functional approach for $pH_2$ is briefly reviewed in Sec. 3, together with the determination of the e-$pH_2$ Hartree interaction. The results are presented and discussed in Sec. 4. Finally, a summary is presented in Sec. 5.

## 2. Capillary approximation

The capillary approximation is found to work fairly well for electron bubbles in liquid helium, especially at low temperatures [11] where the interface separating the electron bubble cavity from the liquid is rather sharp due to the pressure exerted by the electron against the surrounding fluid.

Electron bubbles in hydrogen have been detected long time ago [5]. Their radius have been calculated in [13] using a model characterized by an abrupt interface for the spherical cavity where the electron is localized and taking into account in a simplified way the polarization induced by the electron in the liquid. The model in [13] was supplemented by experimental informations for the electron-$H_2$ scattering length. The e-bubble radius was found to vary between 10 and 12.5 Å (in the temperature range between 20 K and the critical temperature), that is roughly a factor of two smaller than in liquid $^4$He.

In the capillary approximation, the energy of an electron bubble is written as the following sum [18]

$$E = \frac{\pi^2\hbar^2}{2m_e R^2} + 4\pi R^2\gamma + \frac{4\pi}{3}R^3 P - \frac{e^2}{2R}\frac{\epsilon - 1}{\epsilon}\,, \qquad (1)$$

whose four terms correspond, respectively, to the electron energy in an impenetrable spherical well potential of radius $R$, the surface and volume energies and a polarization contribution. In that equation, $m_e$ is the electron mass, $\gamma$ is the surface tension of the liquid-vapor interface, $P$ is the external pressure, and $\epsilon$ is the dielectric constant of $pH_2$. The minimization of the energy with respect to the bubble radius allows one to obtain the equilibrium radius from the equation

$$-\frac{\pi\hbar^2}{4m_eR^5}+\frac{2\gamma}{R}+P+\frac{e^2}{8\pi R^4}\frac{\epsilon-1}{\epsilon}=0\,, \tag{2}$$

which has a solution at any non-negative pressure. Considering for instance $T = 14$ K, were the experimental values of the required inputs are $P = 0.079$ bar (saturated vapor pressure), $\gamma = 2.958$ dyne/cm and $\epsilon = 1.251$ [19] one finds $R_{eq} = 10.7$ Å. It is worth noticing that the polarization energy term has some effect. Had we neglected it, the calculated equilibrium radius would have been $\sim 0.6$ Å larger.

If the liquid is submitted to a tensile strength that brings it below saturated vapor pressure, the electron bubble becomes metastable. A potential energy barrier prevents the bubble explosion. This barrier decreases as the pressure does and eventually vanishes at $P_{expl}$. This is the lowest pressure that can be attained before the electron bubble explodes, that is, expands without limits triggering the phase transition. $P_{expl}$ can be obtained from the conditions $dE/dR = 0$, and $d^2E/dR^2 = 0$, which lead to the following system of coupled equations

$$\begin{aligned}-\frac{\pi^2\hbar^2}{m_eR^3}+8\pi\gamma R+4\pi R^2P+\frac{e^2}{2R^2}\frac{\epsilon-1}{\epsilon}=0\\ \frac{3\pi^2\hbar^2}{m_eR^4}+8\pi\gamma+8\pi RP-\frac{e^2}{R^3}\frac{\epsilon-1}{\epsilon}=0\ .\end{aligned} \tag{3}$$

An analytical solution is obtained if the polarization term is neglected, and we shall use it to quickly illustrate how the cavitation process is affected by the presence of impurities. One gets $R=[5\pi\hbar^2/(8m_e\gamma)]^{1/4}$ and $P=-(8/5)\times[8m_e/(5\pi\hbar^2)]^{1/4}\gamma^{5/4}$. According to this, at $T = 14$ K liquid $pH_2$ becomes macroscopically unstable at $P_{expl} = -28.1$ bar, much higher than the homogeneous cavitation pressure, which is about -70 bar.

The $P_{expl}$ curve obtained from Eqs. (3) is displayed in Fig. 5 as a dot-dashed line. It can be seen that it leads to the unphysical result that $P_{expl} < P_{sp}$ for $T \geq 28$ K. Analogously to the helium case, this failure is related to the presence of a sizeable gas-like region within the electron bubble [11], which cannot be described within the simple capillary approximation. Any improvement in the method used to address cavitation induced by electrons calls for a more realistic description of the bubble-liquid interface, together with using an electron-$pH_2$ interaction that reproduces the energy barrier encountered by an electron entering liquid $pH_2$, much along what has been done for liquid helium [10, 11]. This is the aim of the next Section.

## 3. Density functional for parahydrogen

The basic theoretical ingredient in our approach is the total free energy $F$ of the system written in terms of a temperature-dependent free energy density functional

$f(\rho, T)$

$$F = \int d\mathbf{r} f(\rho, T) \,,$$

where $\rho$ is the $pH_2$ number density. All the required thermodynamical quantities can be obtained from $f(\rho, T)$.

We have recently proposed a free energy density functional for $pH_2$ in the form [16]

$$f(\rho, T) = f_{ni}(\rho, T) + f_c(\rho, T) \,. \tag{4}$$

In this expression, $f_{ni}(\rho, T)$ is the free energy density for an ideal Bose gas (see e.g. [17]) and $f_c(\rho, T)$ is the correlation energy density, which incorporates the correlations induced by the interaction. The correlation part $f_c(\rho, T)$ is written as a polynomial in powers of the density

$$f_c(\rho, T) = a_1(T)\rho^2 + a_2(T)\rho^3 + a_3(T)\rho^4 + a_4(T)\rho^5 \,. \tag{5}$$

The $a_i(T)$ parameters have been fixed so as to reproduce a series of thermodynamics properties along the liquid-gas equilibrium line, namely the equality of pressure and chemical potential of both phases, and the pressure and speed of sound of bulk liquid $pH_2$ at the saturated vapor pressure [20]. In Fig. 1 are plotted the resulting parameters, transformed into dimensionless quantities by means of the standard Lennard-Jones parameters for $pH_2$, namely $\epsilon = 34.2$ K and $\sigma = 2.96$ Å.

As such, this functional is a zero-range one, and finite range effects have been considered in [16] to account for highly inhomogenous configurations, as those appearing when either strongly repulsive electrons or very attractive impurities are present in the liquid. These effects have been included by introducing two modifications into the zero-range DF. Firstly, the term in $\rho^2$ has been replaced with

$$a_1(T)\rho^2 \rightarrow \frac{1}{2}\int \mathrm{d}\mathbf{r}'\rho(\mathbf{r})V(|\mathbf{r}-\mathbf{r}'|)\rho(\mathbf{r}') \,, \tag{6}$$

where $V$ represents the $pH_2$-$pH_2$ interaction screened at distances shorther than a screening parameter $h(T)$. It has a Lennard-Jones form if $r \geq h(T)$ and $V(r) = 0$ otherwise. Secondly, a coarse-grained density is introduced in the remaining terms of the functional in the following way

$$a_i(T)\rho^{1+i} \rightarrow a_i(T)\rho\,\bar{\rho}^i \,, \tag{7}$$

where $\bar{\rho}$ is an average of the density in a small sphere whose radius is of the order of the screening distance. This is a well-known prescription for classical liquids [22], which has been also applied to liquid $^4$He. We refer the reader to [16] for the details. It turns out that the finite-range DF (FRDF) so devised accurately reproduces the experimental surface tension of the liquid-vapor interface all over the phase-coexistence region [21].

Once the density functional $f(\rho, T)$ has been determined, the thermodynamic relationship $P = -f(\rho, T) + \mu\rho$ ($\mu$ being the $pH_2$ chemical potential) allows one to calculate the equation of state in the negative pressure regime, inaccessible to the experimental determination, and to obtain the spinodal line in bulk liquid $pH_2$. In the presence of electrons, the free energy of the system is a functional of the $pH_2$

density $\rho$, the excess electron wave function $\Psi$, and $T$, which we write as

$$F[\rho,\Psi,T] = \int d\mathbf{r}\, f(\rho,T) + \frac{\hbar^2}{2\,m_e}\int d\mathbf{r}\,|\nabla\Psi(\mathbf{r})|^2 + \int d\mathbf{r}\,|\Psi(\mathbf{r})|^2 \int d\mathbf{r}'\,\rho(\mathbf{r}')V_{\mathrm{e-H_2}}(\mathbf{r}-\mathbf{r}')\ , \tag{8}$$

supplementing the FRDF with two more terms that accounts for the electron kinetic energy and the e-p$H_2$ interaction. The latter has been written as a function of the local hydrogen density [23] $\int d\mathbf{r}\,|\Psi(\mathbf{r})|^2 V[\rho(\mathbf{r})]$, where

$$V(\rho) = \frac{\hbar^2 k_0^2}{2\,m_e} + \frac{2\pi\hbar^2}{m_e}\rho\, a_\alpha - 2\pi\alpha e^2\left(\frac{4\pi}{3}\right)^{1/3}\rho^{4/3}\ . \tag{9}$$

$\alpha = 0.801\,\mathrm{\mathring{A}}^3$ is the static isotropic polarizability of a $H_2$ molecule [24], and $k_0$ is determined from the p$H_2$ local Wigner-Seitz radius $r_s = (3/4\pi\rho)^{1/3}$ by solving the equation

$$\tan[k_0(r_s - a_c)] = k_0\, r_s\ . \tag{10}$$

In the above equations, $a_c$ and $a_\alpha$ are the scattering lenghts arising from the hard-core and from the polarization potential. Their sum $a = a_c + a_\alpha$ is equal to the e-$H_2$ total scattering length, which we take equal to the experimental value $a = 0.672$ Å [24]. We fix $a_c$ in such a way to reproduce the experimental value for the total energy $V_0$ of a delocalized electron in bulk liquid p$H_2$, $V_0 = 1.9$ eV at 20 K [7]. We find $a_c = 0.979$ Å, and consequently $a_\alpha \equiv a - a_c = -0.307$ Å.

The above procedure works well for slowly varying density profiles. It lacks however an additional non-local contribution which comes from the long-range polarization energy, namely

$$U_{nl}(\mathbf{r}) = -\frac{\alpha e^2}{2}\int d\mathbf{r}'\frac{\rho(\mathbf{r})-\rho(\mathbf{r}')}{|\mathbf{r}-\mathbf{r}'|^4}\ . \tag{11}$$

Such a term is not usually included in DF calculations due to its computational complexity, and we will neglect it in the present work as well.

To obtain $P_{expl}$ we have proceeded as follows. For given $P$ and $T$ values we have first determined the bulk liquid density $\rho_b$ from the theoretical equation of state. Next, we have solved the Euler-Lagrange equations that result from the variation of the constrained grand potential density $\tilde{\omega}(\rho,\Psi,T) \equiv \omega(\rho,\Psi,T) - \varepsilon|\Psi|^2$, where the grand potential density $\omega(\rho,\Psi,T)$ is derived from Eq. (8)

$$\omega(\rho,\Psi,T) = f(\rho,T) + \frac{\hbar^2}{2\,m_e}|\nabla\Psi|^2 + |\Psi|^2 V(\rho) - \mu\rho\ . \tag{12}$$

It yields

$$\frac{\delta f}{\delta\rho} + |\Psi|^2\,\frac{\partial V}{\partial\rho} = \mu \tag{13}$$

$$-\frac{\hbar^2}{2\,m_e}\Delta\Psi + V[\rho]\Psi = \varepsilon\Psi\ , \tag{14}$$

where $\varepsilon$ is the lowest eigenvalue of the Schrödinger equation obeyed by the electron. These equations are solved in a three-dimensional box using Fast-Fourier techniques [25] imposing that $\rho(\mathbf{r}) = \rho_b$ at the cell boundaries, and that the electron is in the $1s$ state.

Fixing $T$, the above equations are solved for decreasing values of $P$ below the saturated vapor pressure $P_{svp}(T)$. The lower the pressure, the larger the metastable electron cavity. Eventually, a value of the pressure is found for which the procedure is unable to find a metastable e-p$H_2$ configuration, and the electron cavity expands until it reaches the boundaries of the simulation cell. This pressure value numerically defines $P_{expl}$.

As an alternative to the use of the Hartree-type interaction described above, one may take advantage of the large short-range exchange repulsion between the electron and the p$H_2$ molecule, that dominates the long-range polarization attraction, and consider in Eq. (8) a much simpler "contact" interaction

$$V_{\mathrm{e-H_2}}(\mathbf{r} - \mathbf{r}') = \frac{V_0}{\rho_b}\,\delta(\mathbf{r} - \mathbf{r}') \tag{15}$$

whose intensity scales with the liquid density so that it yields the experimental energy barrier $V_0$ encountered by an electron entering liquid p$H_2$, $V_0 = 1.9$ eV at $T = 20$ K [7]. We recall that $\rho_b$ is the bulk p$H_2$ density at such temperature. This type of interaction was already used for liquid $^4$He [10], and the results obtained were found to be very similar to those obtained using the Hartree-type interaction term [11]. We have checked that the results obtained using both type of interactions are indeed very similar also in the case of p$H_2$.

## 4. Results and discussion

Figure 2 shows the calculated e-bubble radii at different temperatures (squares), using the approach described in Sec. 3. The radius is defined as the radial position where the density attains the value $\rho_b/2$, $\rho_b$ being again the bulk liquid density at the investigated temperature. Our results are compared in this figure with the estimates from [13]. At low $T$, where our results are expected to be very similar to the ones obtained within the capillary approximation used in [13], the bubble radius is slightly overestimated, and rather coincides with the value obtained in [13] when the long-range polarization interaction term is omitted. This is in part a consequence of our own neglect of the long-range polarization term Eq. (11).

At higher temperatures the capillary model of [13] breaks down due to the increasing thickness of the liquid-vapor interface in the bubble cavity, which is instead correctly accounted for in our calculations. The density profiles of the p$H_2$ at different temperatures are shown in Fig. 3. It can be seen that the surface thickness of the e-bubble increases as $T$ does.

Figure 4 shows some density profiles illustrating the cavitation process. For each $T$, we show the electron and p$H_2$ profiles corresponding to the stable e-bubble at saturated vapor pressure $P_{svp}$, and those corresponding to the nearly critical bubble at $P_{expl}$.

Finally, we display in Fig. 5 the calculated $P_{expl}$ within the FRDF plus e-p$H_2$ Hartree potential approach and the capillary model as well, together with the saturated vapor pressure, spinodal and homogeneous cavitation curves. It can be seen how the selfconsistent solution of the liquid and excess electron equations circumvents the limitations of the capillary model at high temperatures and yields

sensible results for the e-bubble explosion all over the temperature range where the calculations have been carried out. At lower temperatures, the slight deviations between the FRDF results and the capillary model predictions are due in part to our neglect of the long-range polarization energy term, as discussed previously.

## 5. Summary

We have investivated heterogeneous cavitation in liquid $pH_2$ triggered by the presence of excess electrons. To this end, we have built a Hartree-like electron-parahydrogen interaction, and have used a previously devised finite-range density functional for $pH_2$ that works well in the liquid-vapor equilibrium region.

Our approach allows for a realistic and flexible description of the electron cavity and of the interaction between the electron and the surrounding liquid. It does not impose a priori the density profile of the critical bubble, allowing for a proper description of the process from the saturated vapor pressure down to the spinodal line.

We have found that the critical pressure at which electron bubbles explode is in absolute value about a factor of two smaller than the homogeneous cavitation pressure of liquid $pH_2$. We have also used a capillary model to discuss the onset of electron bubble explosion in liquid $pH_2$, and have discussed the limitations of this model at high temperatures.



## Acknowledgments

This work has been performed under Grants No. FIS2008-00421/FIS and FIS2007-60133 from DGI, Spain (FEDER), and Grant 2009SGR01289 from Generalitat de Catalunya.

## References

[1] C. S. M. Doake and P. W. F. Gribbon, Phys. Lett. A **30**, 251 (1969).
[2] G. G. Ihas and T. M. Sanders Jr., Phys. Rev. Lett. **27**, 383 (1971); G. G. Ihas and T. M. Sanders, in *Proc. 13th Int. Conf. Low Temp. Physics*, edited by K. D. Timmerhaus, W. J. O'Sullivan and E. F. Hammel (Plenum, New York, 1972) Vol. **1**, p. 477.
[3] V. L. Eden and P. V. E. McClintock, Phys. Lett. A **102**, 197 (1984).
[4] F. Aitken, Z.-L. Li, N. Bonifaci, A. Denat and K. von Haeften, Phys. Chem. Chem. Phys. **13**, 719 (2011).
[5] H. R. Harrison and B. N. Springett, Chem. Phys. Lett. **10**, 418 (1971).
[6] G. E. Grimm and G. W. Rayfield, Phys. Lett. A **54**, 473 (1975).
[7] P. B. Lerner and I. M. Sokolov, J. Low Temp. Phys. **95**, 683 (1994).
[8] A. A. Levchenko and L. P. Mezhov-Deglin, JETP Lett. **60**, 470 (1994).
[9] A. V. Berezhnov, A. G. Khrapak, E. Illenberger and W. F. Schmidt, High Temperature **41**, 425 (2003).
[10] J. Classen, C.-K. Su, M. Mohazzab, H. J. Maris, Phys. Rev. B **57** (1998) 3000.
[11] M. Pi, M. Barranco, R. Mayol and V. Grau, J. Low Temp. Phys. **139**, 397 (2005).
[12] H. J. Maris, J. Phys. Soc. Jpn. **77**, 1 (2008).
[13] T. Miyakawa and D. L. Drexter, Phys. Rev. **184**, 166 (1969).
[14] A. A. Levchenko and L. P. Mezhov-Deglin, J. Low Temp. Phys. **89**, 457 (1992).
[15] M. Pi, M. Barranco, J. Navarro and F. Ancilotto, Chem. Phys. (2011), doi:10.1016/j.chemphys.2011.04.033.
[16] J. Navarro, F. Ancilotto, M. Barranco and M. Pi, J. Phys. Chem. A (2011), dx.doi.org/10.1021/jp111996u.
[17] K. Huang, *Statistical Mechanics*, 2nd. ed.; J. Wiley, New York 1987.
[18] D. Konstantinov and H. J. Maris, J. Low Temp. Phys. **121**, 609 (2000).
[19] V. S. Kogan, Y. Y. Milenko and T. K. Grigorova, Physica **53**, 125 (1971).
[20] J. W. Leachman, R. T. Jacobsen, S. G. Penoncello and E. W. Lemmon, J. Phys. Chem. Ref. Data **38**, 721 (2009).
[21] R. D. McCarthy, L. Hord and H. M. Roder, National Bureau of Standards, Monograph **168** (1981).
[22] P. Tarazona, Phys. Rev. A **31**, 2672 (1983).

[23] E. Cheng, M. W. Cole and M. H. Cohen, Phys. Rev. B **50**, 1136 (1994); Erratum *ibid.* **50**, 16 134 (1994).
[24] E. S. Chang, J. Phys. B **14**, 893 (1981).
[25] F. Ancilotto, M. Barranco, E. S. Hernández, A. Hernando and M. Pi, Phys. Rev. B **79**, 104514 (2009).

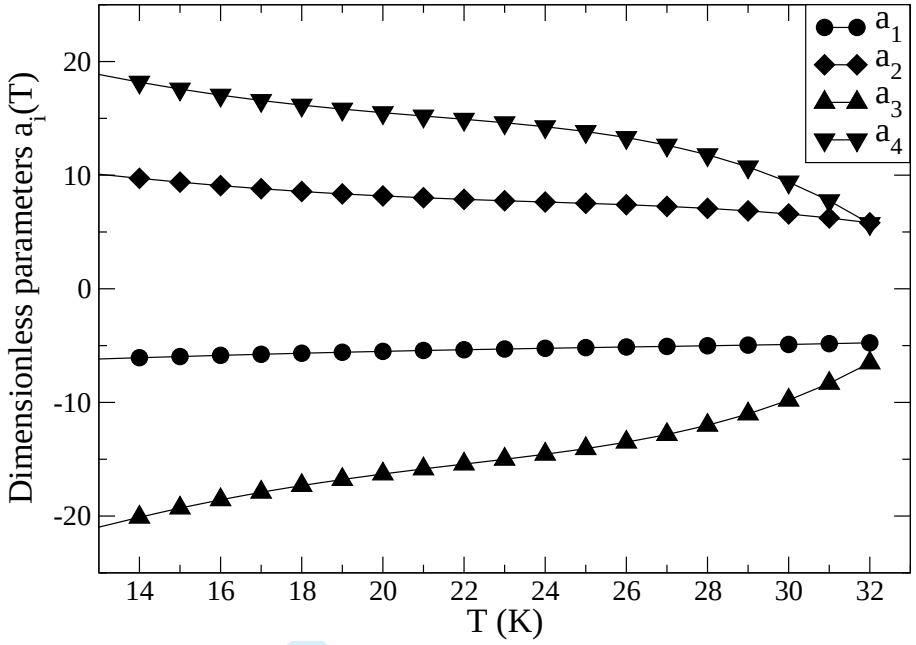


Figure 1. Dimensionless parameters $a_i(T)/(\epsilon\sigma^{3i})$ of the $pH_2$ density functional of Eq. (5) as a function of temperature. The values $\epsilon = 34.2$ K and $\sigma = 2.96$ Å have been used.

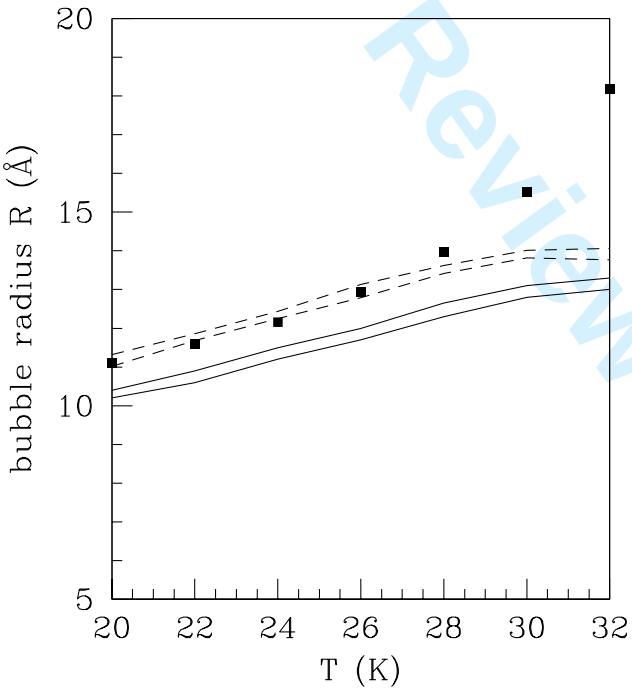


Figure 2. Electron bubble radius at different temperatures. The solid lines show the results of [13] corresponding to two experimental estimates for the electron-$H_2$ scattering length. The dashed lines are the results of [13], where the long-range polarization term has been omitted. The squares show the values calculated using the FRDF with the effective Hartree-type electron-$pH_2$ interaction described in the text.

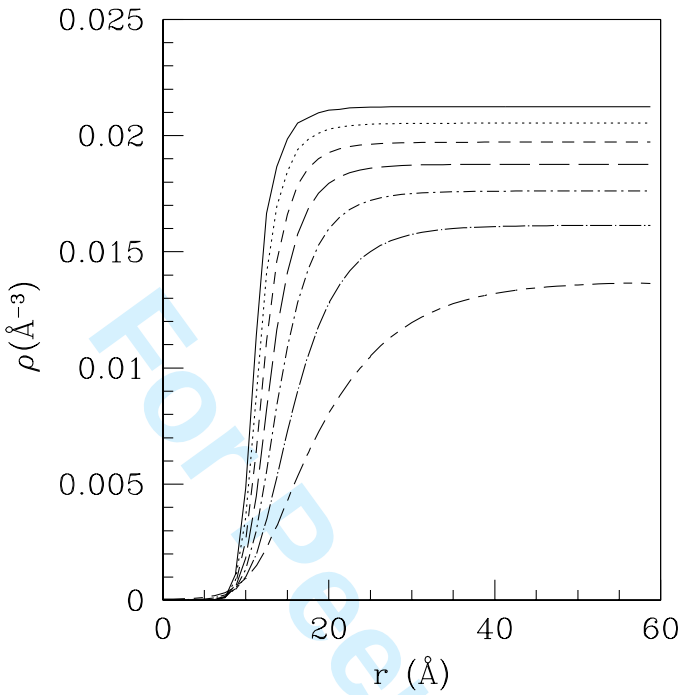


Figure 3. Density profiles of $pH_2$ bubble cavities at saturated vapor pressure conditions and different temperatures. From top to bottom, $T = 20$, 22, 24, 26, 28, 30, and 32 K.

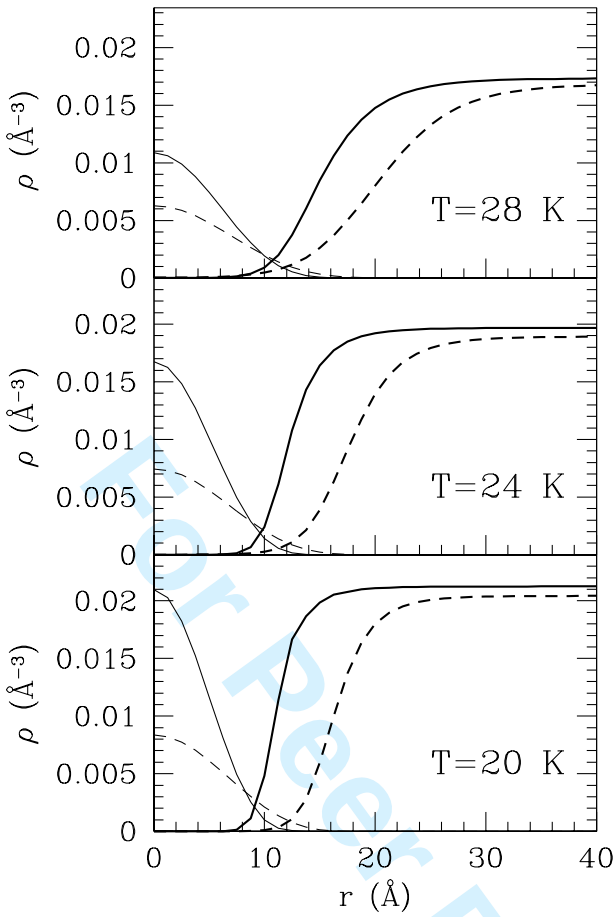


Figure 4. Density profiles of e-bubbles in $pH_2$ for three different values of $T$. For each $T$, we show the electron and $pH_2$ profiles corresponding to the saturated vapor pressure $P_{svp}$ (thin and thick solid lines, respectively), and those corresponding to the nearly critical bubble at $P_{expl}$ (thin and thick dashed lines). The electron probability densities in the panels are shown in a vertical arbitrary scale.

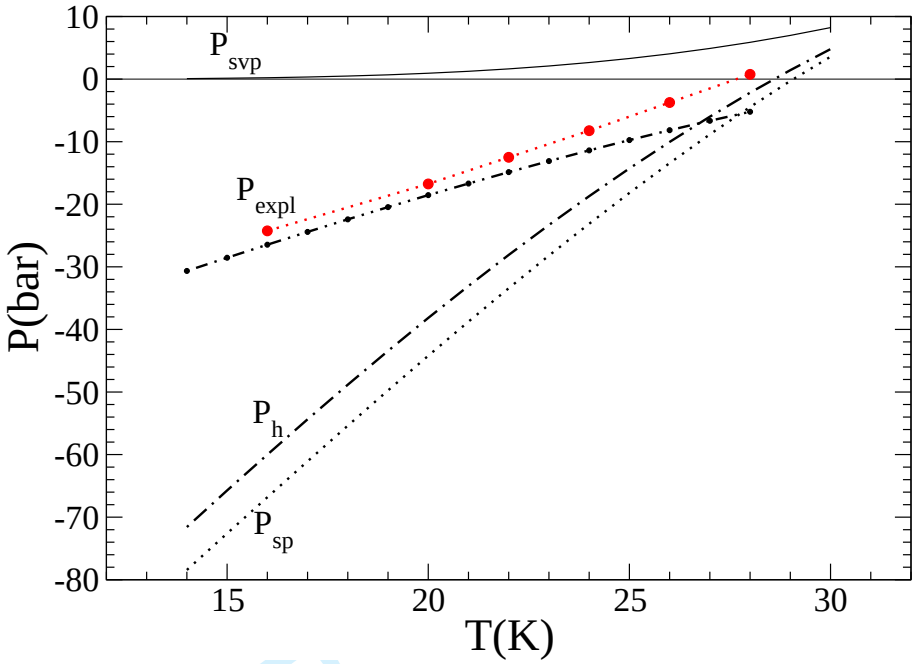


Figure 5. (Color online) Homogeneous cavitation pressure $P_h$ and spinodal pressure $P_{sp}$ as obtained in [16], together with the e-bubble explosion pressure $P_{expl}$ obtained within the capillary approximation (dash-dotted line) and within FRDF theory (dots). In the latter case, the dotted line has been drawn as a guide to the eye. Also shown is the saturated vapor pressure line, $P_{svp}$.